View metadata, citation and similar papers at core.ac.uk
brought to you by CORE
provided by Institute of Transport Research:Publications

Upscaled Synthesis of n- and p-type Thermoelectric Skutterudite single legs by Gas Atomization and Current-assisted Sintering

Christian Stiewe[1], Reinhard Sottong[1], Johannes de Boor[1], Eckhard Müller[1,2]

[1]Institute of Materials Research, German Aerospace Center (DLR), D–51147 Cologne, Germany
[2]Institute for Inorganic and Analytical Chemistry, Justus Liebig University Giessen, Heinrich-Buff-Ring 17, D–35392 Giessen, Germany

Abstract

$CoSb_3$-based Skutterudites are among the best materials for thermoelectric generator (TEG) applications in the intermediate temperature range up to 500 °C. Synthesis of these materials is usually performed on a laboratory scale in materials research. In order to be suitable for an industrial low cost production of TEG technologies capable of delivering large amounts of thermoelectric (TE) materials are needed. A process mastering this challenge is gas atomization, which has been adapted to the requirements of TE materials, in particular $CoSb_3$-based Skutterudites. We found that despite rapid solidification taking place in the atomization process the produced powder material contains only traces of the target Skutterudite phase. Microstructure investigation shows a very fine dispersion on the micrometer scale of CoSb, $CoSb_2$ and Sb phases in the atomized particles, making diffusion paths for the formation of the Skutterudite phase short. This allows the use of short-term heat treatment to achieve almost single phase material of high functional homogeneity. Different thermal post-treatments have been evaluated leading to a content of >98% of the Skutterudite phase in large ingots. Doping and filling by varying the starting composition was applied to tune the materials to n- and p-type conduction, respectively, and led to an increase of their thermoelectric figure of merit *ZT* up to values of 0.9 and 0.72 for n- and p-type material, respectively.

Introduction

Thermoelectric generators are used to convert flowing heat directly into electricity without moving parts or working fluids, thus providing a great potential in applications of waste heat recovery or energy harvesting [1]. In the search for highly efficient thermoelectric materials a new material is usually synthesized on a laboratory scale of a few grams per batch, yielding sufficient material to fabricate some laboratory samples. To bring TEG technology into the market for mass applications like waste heat recovery in vehicles or stationary industrial applications, a large scale production technology of high performance, yet low cost thermoelectric materials is required.

Skutterudites are among the materials with highest conversion efficiency, given by the thermo-electric figure of merit *ZT*, in the relevant temperature range between 250 and 550 °C [2-4]. *ZT* is defined as $ZT=(S^2\sigma/\kappa)\cdot T$, with the Seebeck coefficient *S*, electrical conductivity σ, thermal conductivity κ and the absolute temperature T.

For application, besides the material properties, cost and available quantities play likewise important roles. Here, advanced production methods facilitate a scalable synthesis of Skutterudite materials and have the potential to reduce production cost.

Gas atomization is a commercially widely used method for the large scale production of metal and alloy powders. It combines melting and alloying of the elements, quenching and pulverization into fine powders for subsequent sintering within one single process. For the work presented here a small-scale gas atomizer was used that allows for a material production of 0.5-3 kg of powder per batch which overcomes the threshold from laboratory-style ampoule melting synthesis to a high-throughput one-step powder production method. The method is easily scalable from kilograms to tons per batch and thus allows for a fast and flexible production of thermoelectric material powders as has already been investigated for Bi_2Te_3-Bi_2Se_3 compounds [5] , $Mg_2(Si,Sn)$ [6] and for Ce-filled n-type Skutterudites [7]. In this work we present investigations on undoped and on both p-type and n-type Skutterudites with various filling elements synthesized using gas atomization and subsequent current-assisted sintering. The influence on the phase composition, microstructure and thermoelectric properties of both p- and n-type filled Skutterudite materials are discussed. A moderate chemical purity (3N+) of the original elements has been chosen in order to keep this synthesis route costwise competitive as an industry-relevant production. Results of annealing and sintering effects on materials prepared in the same way are presented elsewhere [8].

Experimental

For the material synthesis a gas atomizer of type Hermiga Mini, PSI Ltd., UK, was used that allows for production quantities of 0.5 – 3 kg of powder per batch, depending on the processed materials´ density. Purified elements (Co: 99.95%, Sb: 99.97%, Fe: 99.98%, Ni: 99.98% all supplied by Sindlhauser Materials GmbH; In: 99.999%, Ce: 99.99%, La: 99.99%, Nd: 99.995% all supplied by AlfaAesar) were treated in a glovebox to prevent oxidation. The Ce-mischmetal (66% Ce, 33% La) was only 99% pure and delivered under air. The elements were weighed and mixed according to the target stoichiometry with 1.5% excess of Sb to compensate for material loss due to evaporation from the melt. The material was heated to 1100 °C in an induction furnace under Argon atmosphere within 1 h. The induction furnace is positioned as part of the upper section (melting chamber) in the atomizer setup. The melt is held at 1100 °C for 10 min before it is released through a ceramic nozzle into a large solidification chamber as the bottom section of the atomizer and then quenched and atomized by a high pressure Argon gas jet into fine droplets. While floating in the inert gas these droplets solidify and transform into micrometer-sized spherical powder particles. The synthesis route is not a complete inert gas process chain, since the gas atomization system used here is not prepared for a loading of the basic elements under inert gas, hence a short exposure to air cannot be excluded. Treatment of the atomized powders in a glove box and hot pressing are done under inert gas or vacuum.

The particle size distribution after atomization was measured in a Beckman Coulter LS 13 320 particle analyzer with ethanol as a working fluid. For structural characterization of the powders as well as of sintered samples, a Siemens Bruker D5000 powder XRD system was employed. The software FULLPROF [9] was used for Rietveld refinement of the XRD data. Powders were compacted in a graphite pressing die with a diameter between 15 and 50 mm using a current-assisted hot press (Dr. Fritsch DSP 510A) at 580 °C and 60 MPa under 0.7 bar of Ar partial pressure to reduce evaporation. The duration of the holding time at maximum temperature was varied between 10 and 30 min in the press.

The temperature-dependent thermal conductivity is calculated from the thermal diffusivity measured with a Netzsch LFA 427, Archimedes' density, and specific heat measured by a Netzsch DSC

404. The temperature-dependent electrical conductivity σ and Seebeck coefficient *S* were measured simultaneously using a custom-built measurement device [10]. S and σ are recorded during subsequent heating and cooling phases of the measurement cycle to obtain information on the functional material stability. Measurement errors are assumed to be 8%, 5%, and 5% for κ, *S*, and σ, respectively. The repeatability of the Seebeck coefficient measurement is better than 5% allowing for the identification of smaller differences between samples; the 5% error mainly accounts for accuracy, meaning an absolute uncertainty of the measured values due to systematic errors [11]. These values sum up to an accuracy of the calculated figure of merit of approx. 20%. Hall measurements were performed at room temperature in a custom-made setup in van der Pauw geometry [12] comparable to the setup discussed in [13]. Hall carrier concentration and mobility were calculated under the assumption of a single carrier type; errors are estimated to be 10% for samples with a Hall carrier concentration $n_H < 3 \cdot 10^{20}$ cm^{-3}. For these with higher carrier concentration the error is estimated to be up to 20% due to lower signal-to-noise ratio. For some of the p-type samples Hall measurements were not possible due to sample breaking during the course of the measurements.

Results and discussion

The influence of the atomization gas jet pressure on the powder particle size has been investigated for undoped Co-Sb with the weighted nominal composition $CoSb_3$. The particle size distributions of the atomized Co-Sb-based powders range from 0.4 to approx. 100 µm with the main volume fraction around 10 µm (see Figure 1). The variation of the atomization gas jet pressure has a significant influence on the mean particle size and shape distribution, thus allowing for a particle size control in a range between main fractions of approx. 20 and 8 µm between 15 and 36 bar gas pressure, respectively.

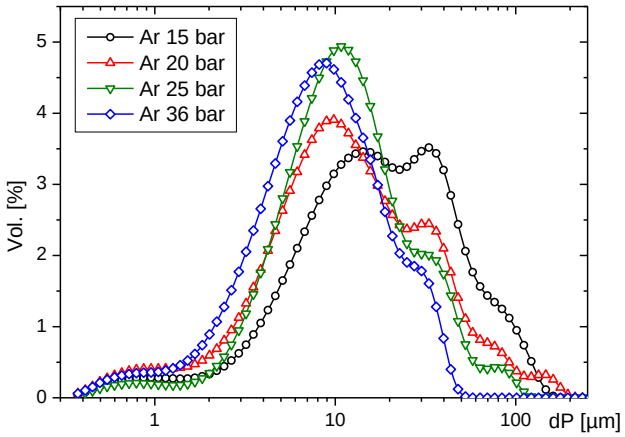

Figure 1: Particle size distribution of Co-Sb-based atomized powders, prepared using different atomization gas pressures

SEM images of atomized powders reveal spherical particle shapes (Figure 2 inset), which is typical for atomized materials, driven by surface tension of the hovering droplets in the inert gas. The spherical shape enhances an easy powder flow e.g. in mechanical feed throughs technological processes. The surfaces of undoped Co-Sb powder particles show a precipitation of seemingly fluffy material, the elemental nature of which could not be identified by EDX because of its fine, open structures. This material might be elemental Sb initially evaporated from the droplets because of its low melting point and high vapor pressure that later re-condensed on the particles´ surfaces. This assumption is supported by the observation of a visible vapor around the melt jet in the atomization chamber before the atomization gas jet sets in. At higher magnification the particle surface shows distinct

polygonal phase regions with a scaling smaller than 1 µm (Figure 2). The chemical nature of these regions is revealed by EDX analyses on cross sections of gas atomized powder particles, as shown in Figure 3 left. The nominal composition in this sample was according to a Ce- and La-filled p-type Skutterudite of $La_{0,053}Ce_{0,099}Co_{0.5}Fe_{0.5}Sb_3$. The micrographs clearly show a multi-phase constitution composed of grains with *M*Sb cores and *M*Sb_2 surrounding (*M* = $Co_{0.5}Fe_{0.5}$) in a Sb matrix with minor regions of *M*Sb_3 decoration the interfaces, and additional La-Sb and Ce-Sb phases. Rapid solidification during gas atomization led to the formation of high temperature *M*-Sb side phases rather than establishing the desired Skutterudite phase in accordance to the phase diagram.

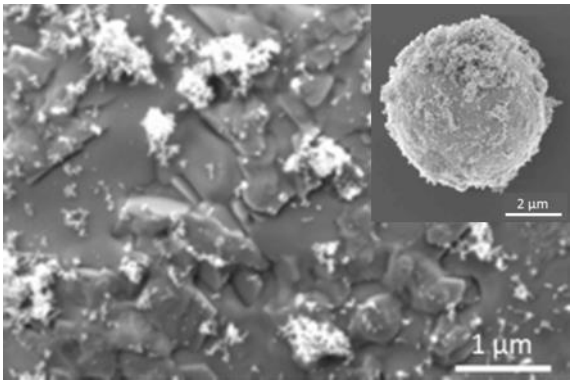

Figure 2: SEM micrographs of atomized Co-Sb-based powder particle surfaces; inset: Spherical shape of the produced particles

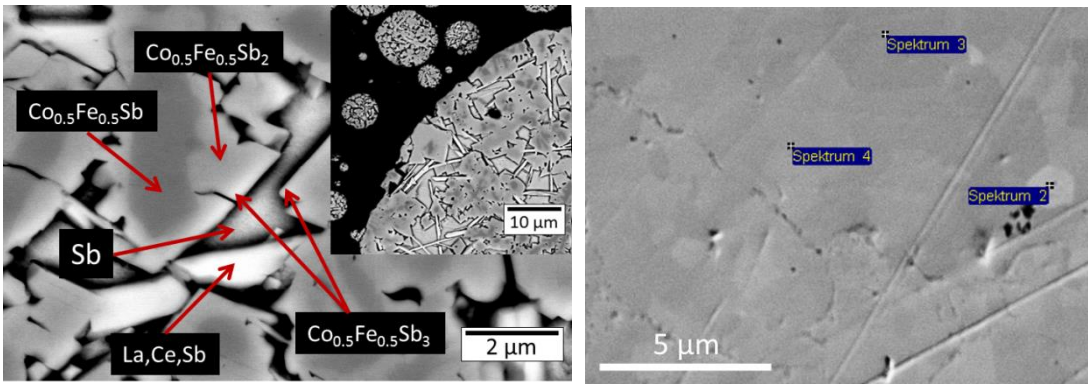

Figure 3: Left: SEM micrographs and element analysis on cross sections of gas atomized Co-Fe-Sb-based powder particles with La and Ce addition as filling elements (nominal composition $La_{0,053}Ce_{0,099}Co_{0.5}Fe_{0.5}Sb_3$); Right: Hot pressed pellet from the same material; labels indicate location of point IDs by EDX (Table 1)

Table 1: Results of the EDX analyses of point IDs indicated in Figure 3 (right)

at.-%	Fe	Co	Sb	La	Ce
Spektr. 2	10.5	11.6	75.3	0.5	2.1
Spektr. 3	10.7	10.8	75.2	1.2	2.1
Spektr. 4	10.4	10.4	76.3	1.0	1.9

The Co-Sb phase diagram shows the peritectic segregation into liquid Sb and CoSb during cooling, which at lower temperatures partly converts into the $CoSb_2$ γ phase, which is stable up to 936 °C and later into the $CoSb_3$ δ phase, which is stable up to 874 °C [14]. Since the diffusion at this comparably low temperature is very slow and the duration in this temperature range is short during passive

cooling of the droplets, only a small content of δ phase is found at the boundaries between the dark gray areas and the Sb matrix in Figure 3 left.

Therefore, alike to the established ampoule melt-quench route, a thermal post-treatment of the quenched material was necessary to transform the material into the desired MSb$_3$ phase. Several processes have been tested on undoped Co-Sb powder from the same atomization run such as ball-milling, heat-treatment of the as-atomized powders in a furnace or during hot pressing. The results of the XRD phase analyses are shown in Figure 4.

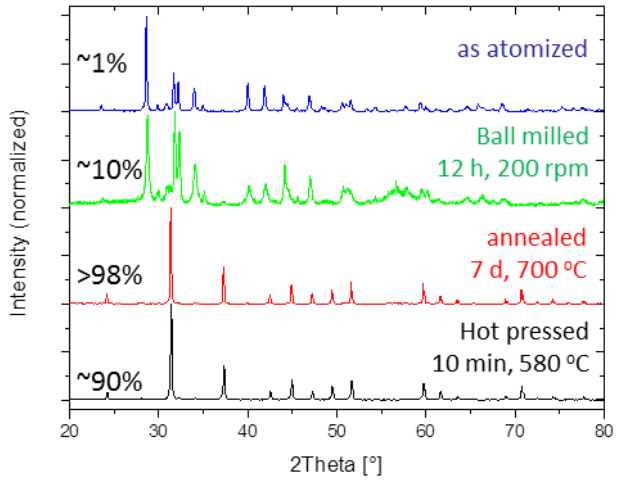

Figure 4: XRD patterns and results of the phase analysis of the atomized powders of undoped Co-Sb material before and after different post-processings. The content of the Skutterudite phase is given in vol.-%.

The as-atomized powder contains hardly any Skutterudite phase. The formation of $CoSb_3$ by mechanical alloying is known from literature [15] and the synthesis of Skutterudite phase from elemental powder mixtures by ball milling has been investigated [16]. A maximum Skutterudite content of 75% was reached there after 8 h of ball milling at 300 rpm. In our work the starting material is already a fine powder with a very fine distribution of the predecessor phases, so a more gentle approach with 12 h of ball milling of gas atomized powder in a planetary ball mill at 200 rpm has been tried. The content of Skutterudite phase could be increased to merely about 10%, which is comparable with literature results on ball milling of ingots quenched from the melt [17]. For comparison, a long-term heat treatment of atomized powder sealed in a quartz ampoule under Ar for 7 days at 700 °C (comparable to usual procedure) for ingots from the conventional melt-quench synthesis) was tested and confirmed the feasibility of getting single phase material from gas atomization. The powder contained up to about 98% of Skutterudite phase, with an experimental error of ±1%, with side phases of $CoSb_2$, possibly because of Sb loss during the melting process. A heat treatment with longer duration and at higher temperature did not lead to higher phase content. However, this route would be too time-consuming and laborious for an industrial mass production technique. As a much faster alternative, a short-term heat treatment related to the current-assisted sintering for 10 min not only provides a compacted pellet of high density but also leads to the formation of approx. 90% of the Skutterudite phase in the pellet. In further tests this phase content could be increased to >98% after a hot pressing at 580 °C for 20 min. These results were obtained with undoped and unfilled Co-Sb material. When using these process parameters for In-filled material In_xCoSb_3 about 96% of Skutterudite phase could be achieved complemented by impurities of In-Sb and $CoSb_2$ whereas for the Ce- and La-filled $(Ce,La)_xCoSb_3$ about 95% of Skutterudite phase with

side phases of rare earth antimonides and $FeSb_2$ have been found (see Table 2). The needle-like rare earth antimonides in the as-atomized powders are high temperature stable (up to 1130 °C in case of Ce, In) and mostly consumed during the heat treatment by hot pressing. Since XRD of the hot pressed pellets showed the presence of residual side phases that are not in the SEM/EDX analysis in different locations of hot pressed pellets (Figure 3 right and Table 1), a very fine side phase distribution below the spatial?? resolution of the SEM must be assumed.

In ingots from melt synthesis Skutterudite phase contents of 75-80 vol.-% are reported before heat treatment and of 93 vol.-% and >98 vol.-% after 2 and 7 days treatment at 700 °C, respectively [18]. The different durations of heat treatment necessary for the homogenization of melt ingots compared to the relatively short duration for atomized powders can be attributed to the different characteristic lengths of the phase mixtures, governing the transformation rate. As seen in Figure 3 for atomized powders a phase mixture with a scaling of about 2 µm around Sb precipitates in one particle is visible, whereas for quenched melt ingots these lengths are typically in the range of 50-100 µm, depending on the cooling rate upon solidification. Longer separation lengths between the phases require longer homogenization times by diffusion.

Skutterudites were synthesized by gas atomization and hot pressing as n-type $CoSb_3$-based and p-type $(Co,Fe)Sb_3$-based materials with different filling elements such as In, Ce and MM (mischmetal: 66% Ce, 33% La) to reduce the thermal conductivity and tune the electrical properties, hence increase the figure of merit. It is well known that both structure filling and altering the Co/Ni or Co/Fe ratio changes the doping level in Skutterudites [19]. As can be seen from Table 2 the addition of the filler leads to an increase in carrier concentration for both n- and p-type samples in the range of 10^{19} cm^{-3} – 10^{20} cm^{-3}, partially surpassing the reported optimum carrier concentration in the order of 10^{20} cm^{-3} or 0.5 charge carriers per unit cell independent on the filling element for p- and n-type Skutterudite, respectively [20].

Table 2: Nominal composition and room temperature Hall and XRD data ($M=Co_{1-x}Ni_x$ for n-type and $M=Co_{1-y}Fe_y$ for p-type samples).

Composition	Type	n_H [$10^{19}cm^{-3}$]	σ [$S \cdot cm^{-1}$]	μ_H [$cm^2 \cdot V^{-1} \cdot s^{-1}$]	a [Å] Kieftite	Kieftite vol.-%	MSb_2 vol.-%	MSb vol.-%	Sb vol.-%	other vol.-%	RWP
$In_{0.05}CoSb_3$	n	7.4	825	70	9.043953	98	1	<1		<1	8.998
$In_{0.06}CoSb_3$	n	13.6	1030	47	9.042371	97	1	<1	<1	1	9.324
$In_{0.025}Co_{0.9}Ni_{0.1}Sb_3$	n	39.0	1010	16							
$In_{0.05}Co_{0.93}Ni_{0.07}Sb_3$	n	26.0	775	19							
$In_{0.035}Co_{0.96}Ni_{0.04}Sb_3$	n	16.9	570	21	9.039727	96	2	<1	<1	1	7.464
$MM_{0.025}Co_{0.67}Fe_{0.33}Sb_3$	p										
$MM_{0.07}Co_{0.62}Fe_{0.38}Sb_3$	p	11.6	425	23	9.069631	97	2	<1	<1	<1	17.13
$MM_{0.15}Co_{0.5}Fe_{0.5}Sb_3$	p				9.087153	96	1	1	<1	<1	13.57
$Ce_{0.1}Nd_{0.1}Ni_{0.08}Fe_{0.92}Sb_3$	p	120.0	1770	9	9.127059	95	3	<1	1	<1	17.11
$La_{0.053}Ce_{0.099}Co_{0.5}Fe_{0.5}Sb_3$	p	45.0	620	9	9.090162	96	2	<1	<1	1	13.55

The structural filling limit depends on the certain element and on the substitution level for Co. For example the maximum filling of In in n-type In_xCoSb_3 is reached with $x = 0.05$ [21], while for Ce or La in p-type $(Ce,La)_xFeSb_3$ it is $x = 0.225$ [22]. The thermoelectric properties of n-type $In_xCo_{1-y}Ni_ySb_3$ and p-type $MM_xCo_{1-y}Fe_ySb_3$ were investigated. The results for Seebeck coefficient, electrical and thermal conductivity of n- and p-type Skutterudites are presented in Figure 5. For the n-type material an

increase of the In content increases the electrical conductivity and reduces the Seebeck coefficient in agreement with the measured increasing charge carrier density. The n-type samples show consistently the opposing trends of carrier concentration and Seebeck coefficient. The electrical conductivities increase with increasing carrier concentration, however not proportional to n_H due to a massive reduction of the carrier mobility for the Ni-containing samples. A reduction of the mobility with increasing carrier concentration is expected due to increasing carrier-carrier and impuritiy scattering in agreement to the results obtained on Ni-substituted $CoSb_3$-Skutterudites [23]. The samples with low mobilities exhibit weaker decrease of the electrical conductivity with increasing temperature indicating an additional scattering mechanism that is more effective at lower temperatures as likely cause. Scattering of charge carriers on secondary phases at the grain boundaries, e.g. oxides, in addition to the usual electron phonon scattering, could lead to the observed behavior [24], however, further microstructural characterization is required to verify this hypothesis. Similarly, for the p-type samples also low mobility values are obtained for highly doped samples again in agreement to literature data and explaining the partially poor electrical conductivities [25].

P-type material of $Co_{0.5}Fe_{0.5}Sb_3$ has been prepared filled both with commercial Ce-Mischmetal and a mixture of Ce:La=2:1 from highly purified elements, respectively, for comparison. The lower electrical conductivity of the first material might be explained by residual oxides and impurities, since the commercial MM was not oxide-free. The Seebeck coefficient of these samples suggests a lower charge carrier density in the MM-sample, which is mainly determined by the Fe-content in p-type Skutterudites, hence partial oxidation of Fe could lead to a lower substitution level than expected.

While the obtained values for the Seebeck coefficient and thermal conductivity for all gas atomized materials are comparable to literature values reported for similar compositions, the electrical conductivity of the gas atomized materials are only about half of the literature data for comparable compositions [26-28]. Hall effect data reveals reduced charge carrier densities in the gas atomized material, while at the same time lower mobilities compared to literature data [18, 29]. This may be caused by side phases of oxides decorating the grain boundaries or high-temperature stable antimonides. However, no clear evidence for such side phases could be seen from XRD and SEM investigations.

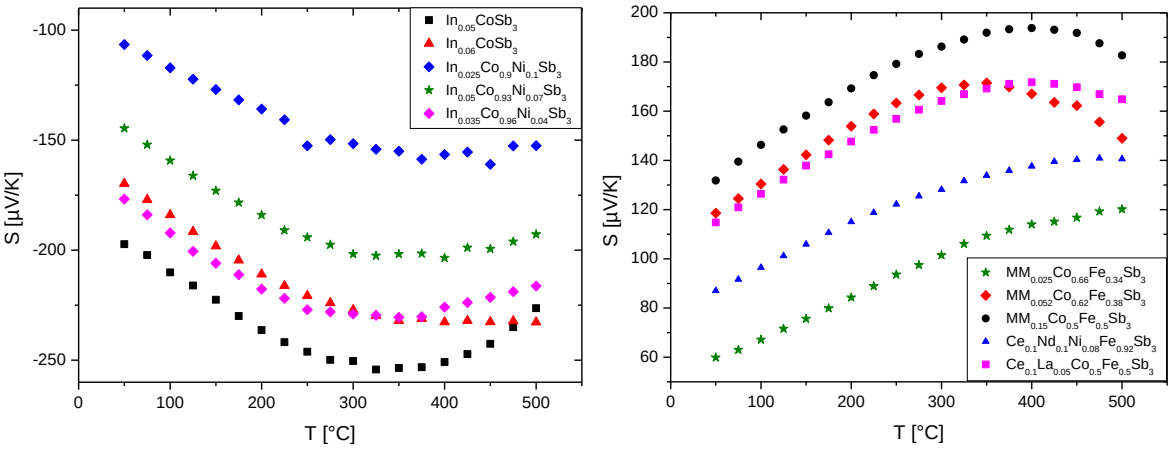

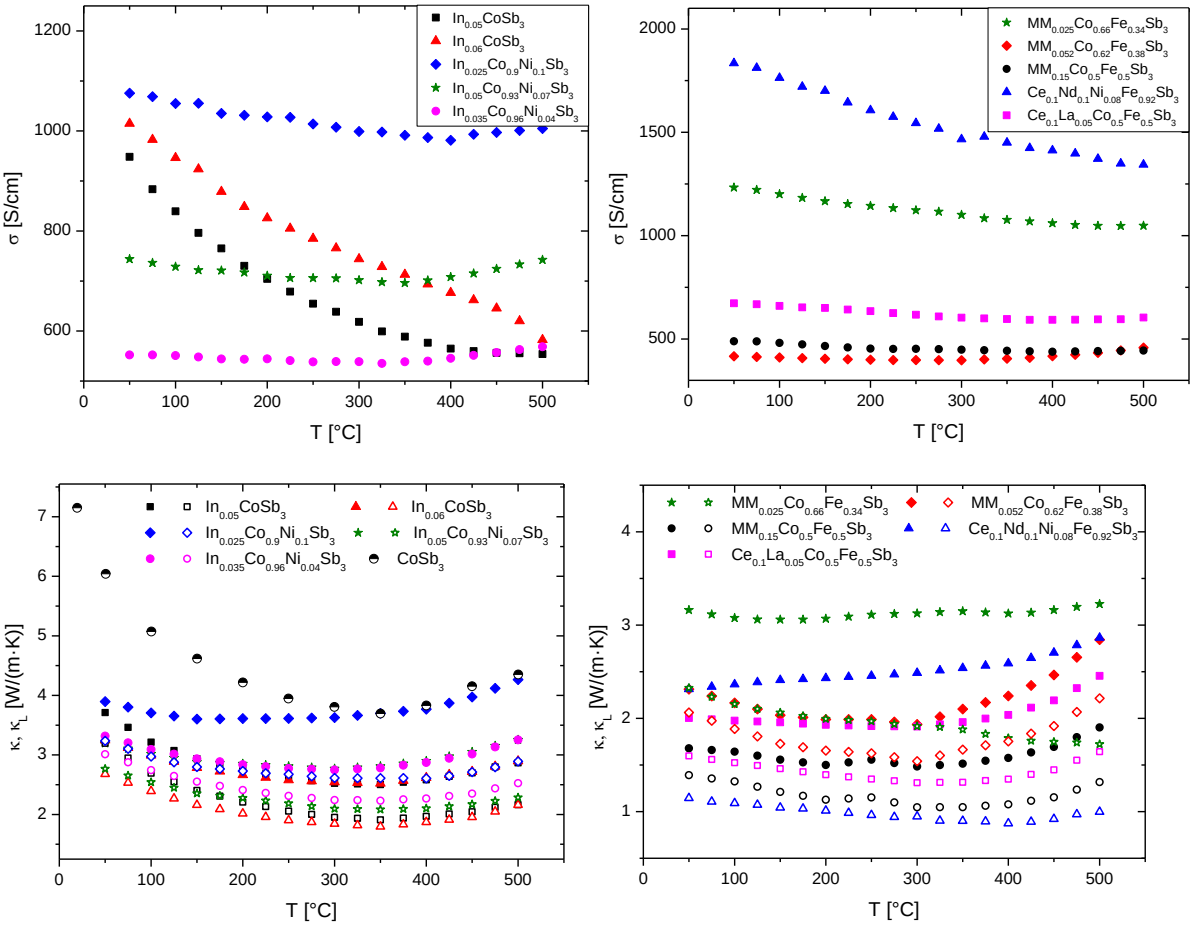

Figure 5: Temperature dependence of Seebeck coefficient, electrical and thermal conductivity (including the lattice contribution) for n-type (left) and p-type (right) Skutterudites prepared from gas atomized powders.

The lattice contribution to the thermal conductivity κ_L (see Figure 5) is estimated using the Wiedemann–Franz law ($\kappa_L = \kappa - L\sigma T$) with the Lorentz number L calculated using the Seebeck coefficient data as $\kappa_L = 1 + \exp(-|S|/166)$ [30]. The thermal conductivity of unfilled $CoSb_3$ prepared by gas atomization is given for comparison, almost identical to the lattice contribution in $CoSb_3$ because of its low electrical conductivity. The lattice thermal conductivity is strongly reduced in all filled materials with smaller values for higher In and Ni contents in the n-type material, with the stronger influence of In than Ni and even slightly increased κ_L with maximum investigated Ni substitution of 10% for Co. The reduction in κ_L by the In filling is more sensitive at lower filling level, reaching a minimum of 1.5 W/(m·K) at 350 °C for $In_{0.06}CoSb_3$. In the p-type material the high-level substitution of Co by Fe allows for a higher structural filling limit, as discussed before, hence lower lattice thermal conductivities are reached compared to the n-type material. Generally, κ and κ_L get smaller with increased filling level both for MM and Ce/La, reaching a minimum κ_L of 0.9 W/(m·K) at 400 °C for $Ce_{0.1}La_{0.05}Co_{0.5}Fe_{0.5}Sb_3$ comparable to literature data of highly Ce- or Yb-filled Skutterudites [31]. An even higher filling was tested with $Ce_{0.1}Nd_{0.1}Ni_{0.08}Fe_{0.92}Sb_3$, but the thermal conductivity could not be reduced more.

The measured thermoelectric properties combine to the values of the figure of merit as shown in Figure 6. For the tested compositions increasing the amount of In filling in the n-type material raises the *ZT* values, whereas Ni substitution for Co contradicts this behavior as already seen in unfilled Ni-doped Skutterudites [23], resulting in a maximum *ZT* of 0.9 at 390 °C for $In_{0.05}CoSb_3$. For the p-type

material the highest *ZT* values are reached for a substitution of Co by Fe by around 50% for the samples investigated here. Depending on the filling element different optimum Co:Fe ratios are reported, ranging from 5:3 for Ce filling to 1:7 for La-MM ([32, 33]). Again the higher filling fraction of mischmetal increases *ZT*, resulting in a maximum of 0.7 at 410 °C for $MM_{0.15}CoSb_3$. In both cases the formulae represent the nominal compositions; the actual filling level could not be refined from XRD measurements.

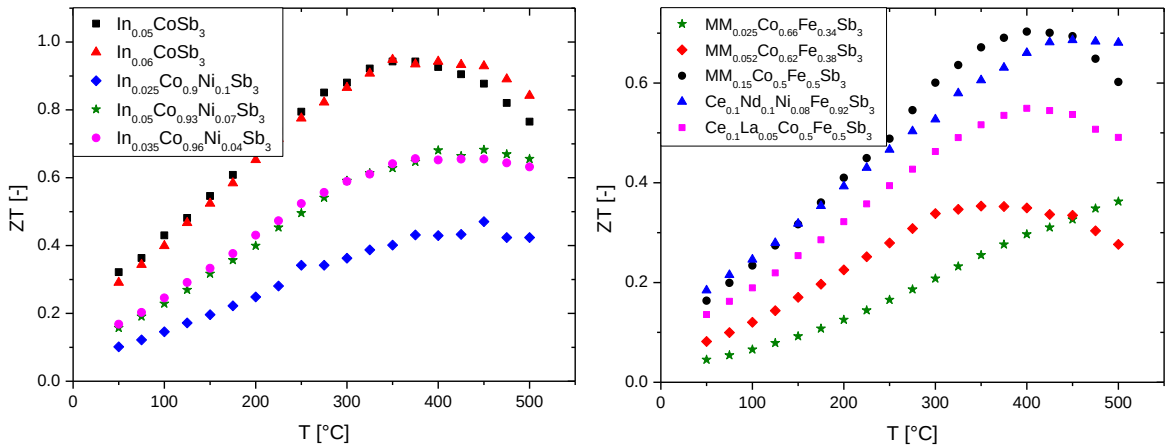

Figure 6: Temperature dependent thermoelectric figure of merit of n- (left) and p-type (right) Skutterudite materials prepared by gas atomization

The technique of gas atomization provides sufficient amounts of material for the fabrication of large ingots, used for the production of TE single legs on an industrial-sized scale. Here ingots of 50 mm in diameter, 35 mm in thickness and about 0.5 kg each were prepared by hot pressing of gas atomized powders. A multi-filament wire saw was used for cutting the ingots into wafers of precise thickness, determining the length of the single legs after separation of the wafers into blocks by a precision wafer saw. Figure 7 shows pictures after each of these processing steps. Before this separation step into TE legs the base faces of the wafers can be coated with metal layers acting as diffusion barriers and adhesion layers in the bonding process for a TE module setup. The combination of these down-the-line steps with the gas atomization synthesis allows for large-scale production of Skutterudite-based TEG.

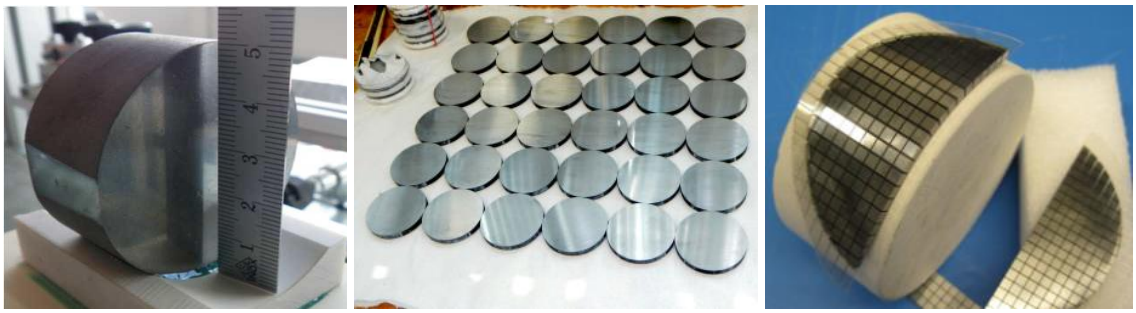

Figure 7: Hot pressed Skutterudite ingot of 50 mm Ø (left), cut into wafers (middle) and finally into single legs (right)

Conclusion

Gas atomization can be used in combination with current-assisted hot pressing to produce p- and n-type Skutterudite single legs. In comparison to an ampoule melt synthesis this technique allows for

large material quantities in comparably short time, making it suitable for an industrial application. The achieved thermoelectric figure of merit of these materials (0.9 for n-type, 0.7 for p-type) is about half of the maximum values reported in the literature for similar compositions. The difference can be attributed mainly to lower electrical conductivities. Hall effect measurements showed lower charge carrier densities and at the same time reduced charge carrier mobilities for the gas atomized materials compared to literature data. The lower doping/filling efficiency, the reduced mobility and the observed changed temperature dependence of the electrical conductivity for samples with high filling levels are plausibly explained by the existence of side phases like oxides or high-temperature stable antimonides. These could be the result of the starting low grade elements of technical purity and the used gas atomization system, which cannot be loaded under complete inert atmosphere. However, no evidence of such side phases could be seen from XRD or SEM. Our results prove the possibility of Skutterudites fabrication by gas atomization with moderate thermoelectric properties and moreover give indications how to improve these further.

Literature

1. *Thermoelectrics Handbook: Macro to Nano* 1ed, ed. D.M. Rowe2005, Boca Raton: CRC Press, Taylor & Francis. 1008.
2. Rull-Bravo, M., et al., *Skutterudites as thermoelectric materials: revisited.* RSC Advances, 2015. **5**(52): p. 41653-41667.
3. Sales, B.C., *Filled Skutterudites*, in *Handbook on the Physics and Chemistry of Rare Earths*, J.C.G.B. K.A. Gschneidner and V.K. Pecharsky, Editors. 2003, Elsevier. p. 1-34.
4. Biswas, K., et al., *High-performance bulk thermoelectrics with all-scale hierarchical architectures.* Nature, 2012. **489**: p. 414-418.
5. Kim, H.-S. and S.-J. Hong, *Thermoelectric properties of n-type 95%Bi_2Te_3–5%Bi_2Se_3 compounds fabricated by gas-atomization and spark plasma sintering.* Journal of Alloys and Compounds, 2014. **586**(Supplement 1): p. S428-S431.
6. Bernard-Granger, G., et al., *Microstructure investigations and thermoelectrical properties of an N-type magnesium–silicon–tin alloy sintered from a gas-phase atomized powder.* Acta Materialia, 2015. **96**(Supplement C): p. 437-451.
7. Tanahashi, H., et al. *Optimization of $CoSb_3$ based Skutterudite TE-Materials Prepared by Gas Atomizing and Sintering*. in *19th International Conference on Thermoelectrics*. 2000. Cardiff, Wales: Babrow Press.
8. Schmitz, A., et al., *Annealing and sintering effects in thermoelectric Skutterudites synthesized by gas atomization.* physica status solidi (a), 2016. **213**(3): p. 758-765.
9. Carvajal, J., *FULLPROF: A Program for Rietveld Refinement and Pattern Matching Analysis.* Abstracts of the Satellite Meeting on Powder Diffraction of the XV Congress of the IUCr, 1990.
10. de Boor, J., et al., *High-Temperature Measurement of Seebeck Coefficient and Electrical Conductivity.* Journal of Electronic Materials, 2013. **42**(7): p. 1711-1718.
11. de Boor, J. and E. Muller, *Data analysis for Seebeck coefficient measurements.* Review of Scientific Instruments, 2013. **84**(6): p. 065102.
12. van der Pauw, L.J., *A method of measuring specific resistivity and Hall effect of discs of arbitrary shape.* Philips Research Reports, 1958. **13**: p. 1-9.
13. Borup, K.A., et al., *Measuring thermoelectric transport properties of materials.* Energy & Environmental Science, 2015. **8**(2): p. 423-435.
14. Predel, B., *Co-Sb (Cobalt-Antimony)*, in *Landolt-Börnstein - Group IV Physical Chemistry - Ca-Cd – Co-Zr* 1993, SpringerMaterials.

15. Yang, J., et al., *Synthesis of $CoSb_3$ Skutterudite by mechanical alloying.* Journal of Alloys and Compounds, 2004. **375**(1): p. 229-232.
16. Zhang, L., et al., *$MmFe_4Sb_{12}$- and $CoSb_3$-based nano-Skutterudites prepared by ball milling: Kinetics of formation and transport properties.* Journal of Alloys and Compounds, 2009. **481**(1-2): p. 106-115.
17. Jie, Q., et al., *Fast phase formation of double-filled p-type Skutterudites by ball-milling and hot-pressing.* Physical Chemistry Chemical Physics, 2013. **15**(18): p. 6809-6816.
18. Sesselmann, A., *Investigation on the Thermoelectric and Structural Properties of Cobalt-Antimony based Skutterudites and Modifications with Indium and Rare-Earth Elements*, in *Ph.D. thesis at Mathematisch-Wissenschaftliche Fakultät* 2012, Universität Augsburg.
19. Chen, B., et al., *Low-temperature transport properties of the filled Skutterudites $CeFe_{4-x}Co_xSb_{12}$.* Physical Review B, 1997. **55**(3): p. 1476-1480.
20. Tang, Y., *Thermoelectric Skutterudites: Why and how high zT can be achieved*, in *Ph.D. thesis at Engineering and Applied Science Division* 2016, California Institute of Technology.
21. Visnow, E., et al., *On the True Indium Content of In-Filled Skutterudites.* Inorganic Chemistry, 2015.
22. Qiu, P.F., et al., *High-temperature electrical and thermal transport properties of fully filled Skutterudites RFe_4Sb_{12} (R = Ca, Sr, Ba, La, Ce, Pr, Nd, Eu, and Yb).* Journal of Applied Physics, 2011. **109**(6): p. 063713.
23. Kim, I.-H. and S.-C. Ur, *Electronic transport properties of Ni-doped $CoSb_3$ prepared by encapsulated induction melting.* Metals and Materials International, 2007. **13**(1): p. 53-58.
24. de Boor, J., et al., *Microstructural effects on thermoelectric efficiency: A case study on magnesium silicide.* Acta Materialia, 2014. **77**(0): p. 68-75.
25. Kim, I.-H. and S.-C. Ur, *Electronic transport properties of Fe-doped $CoSb_3$ prepared by encapsulated induction melting.* Materials Letters, 2007. **61**(11): p. 2446-2450.
26. Rogl, G., et al., *In-doped multifilled n-type Skutterudites with ZT = 1.8.* Acta Materialia, 2015. **95**: p. 201-211.
27. Alboni, P.N., et al., *Thermoelectric properties of $La_{0.9}CoFe_3Sb_{12}$-$CoSb_3$ Skutterudite nanocomposites.* Journal of Applied Physics, 2008. **103**(11): p. 113707.
28. Rogl, G. and P. Rogl, *Skutterudites, a most promising group of thermoelectric materials.* Current Opinion in Green and Sustainable Chemistry, 2017. **4**(Supplement C): p. 50-57.
29. Qiu, P., et al., *Enhancement of thermoelectric performance in slightly charge-compensated $Ce_yCo_4Sb_{12}$ Skutterudites.* Applied Physics Letters, 2013. **103**(6): p. 062103.
30. Chai, Y.W., T. Oniki, and Y. Kimura, *Microstructure and thermoelectric properties of a $ZrNi_{1.1}Sn$ half-Heusler alloy.* Acta Materialia, 2015. **85**: p. 290-300.
31. Liu, R., et al., *Composition optimization of p-type Skutterudites $Ce_yFe_xCo_{4-x}Sb_{12}$ and $Yb_yFe_xCo_{4-x}Sb_{12}$.* Journal of Materials Research, 2011. **26**(15): p. 1813-1819.
32. Tang, X., et al., *Synthesis and thermoelectric properties of p-type- and n-type-filled Skutterudite $R_yM_xCo_{4-x}Sb_{12}$ (R:Ce,Ba,Y; M:Fe,Ni).* Journal of Applied Physics, 2005. **97**(9): p. 093712.
33. Dahal, T., et al., *Transport and mechanical properties of the double-filled p-type Skutterudites $La_{0.68}Ce_{0.22}Fe_{4-x}Co_xSb_{12}$.* Acta Materialia, 2016. **117**: p. 13-22.